Jurnal Kimia Unand
Published by Chemistry Departement
Universitas Andalas

ISSN (online) : 3026 - 2933
ISSN (print) : 2303 - 3401

Synthesis of Hydrophobic Coatings on Concrete Surface Using Organosilicone/Tio₂ and Organosilicone/Carbon-Based Materials

Diana Vanda Wellia[a*], Rahma Yanni[a], Benny Hidayat[b]

[a]Department of Chemistry, Andalas University, Padang 25163, Indonesia
[b]Department of Civil Engineering, Andalas University, Padang 25163, Indonesia
*Corresponding author: nandadiana@sci.unand.ac.id

Abstract

Surface coating methods provide protection for porous concrete surfaces against water diffusion, which can otherwise lead to structural damage and a reduction in concrete's service life. This study aims to assess the impact of varying quantities of biosynthesized TiO_2 and coconut shell-derived carbon on concrete surface hydrophobicity and to compare their effectiveness in enhancing it. SEM analysis confirmed that the organosilicone-based hydrophobic coating with 0,20 g of TiO_2 and 0,20 g of carbon was uniformly distributed, covering micropores, and increasing concrete surface roughness. EDS analysis indicated a decrease in the Ca element peak and the absence of elements like Al, Fe, and K, validating the success of the concrete surface coating. FTIR analysis revealed the emergence of new absorption bands, such as 2963 cm^{-1} (aliphatic C-H bonds of organosilicone) and 477 cm^{-1} (Ti-O bonds), on the hydrophobic concrete surface. Contact angle measurements demonstrated hydrophobic behavior, with the B/Organosilicone/TiO_2 sample exhibiting an angle of up to 122,4º and the B/Organosilicone/C sample up to 138,3º. Consequently, carbon derived from coconut shell waste emerges as a viable alternative for hydrophobic surface applications due to its superior hydrophobicity properties compared to TiO_2.

Keywords

hydrophobicity
concrete
organosilicone
TiO_2
carbon (not capitalized)

Received: October 2025
Revised: October 2025
Accepted: November 2025
Available online: November 2025

1. Introduction

Concrete is a popular construction material due to its strength, workability, and long-term durability[1]. Although concrete has many advantages, its hygroscopic nature and rich porosity make it susceptible to damage due to water diffusion which can reduce its mechanical strength and durability[2]. Water is a detrimental factor for concrete construction, especially in areas with high humidity[3]. Water can penetrate the concrete surface through the porosity present in concrete as a result of thermal changes in the concrete structure exposed to external environmental conditions. The presence of water can also promote the growth of microorganisms, which further deteriorate the concrete surface. Over time, the formation of micro-cracks can compromise the dimensional stability and structural integrity of concrete, ultimately shortening its service life[2,4].

There are several methods of protecting concrete surfaces including hydrophobic impregnation, surface coating, and pore blocking. The surface coating method is widely used due to its effectiveness and ease of application[2]. Hydrophobic coatings are applied to resist water diffusion as a solution in improving the durability of concrete, ensuring the desired service life, and reducing the maintenance cost of concrete structures[5,6]. Coatings can be made from various materials such as silicone, acrylic, epoxy, and polyurethane. These materials form a protective layer on the concrete surface that repels water and other liquids, but these materials alone are not sufficient to provide hydrophobicity and are less economical[1,2].

TiO_2 and carbon particles are some of the additives that can be used to increase the hydrophobicity of a surface. TiO_2 nanoparticles are used because they can improve surface roughness in hydrophobic surface applications. TiO_2 nanoparticles are widely utilized due to their chemical stability, practical applicability, and non-toxicity. Their applications span various fields including catalysis, photocatalysis, antibacterial materials, and building construction-particularly as self-cleaning nanocoatings that enhance surface durability and performance[7]. Carbon particles are nonpolar and their rough

surface allows carbon-containing materials to have high hydrophobicity. Coconut shell waste, which has a high carbon content (49.86 %), was chosen as one source of carbon as an additive for hydrophobic coatings on concrete surfaces because in many countries this waste has not been optimally utilized as a high-value product[8,9].

Zhu et al. have reported that silicone-based coatings exhibit strong water-repellent effects when applied to both normal and recycled aggregate concrete, reducing water absorbency by approximately 60% for each type of aggregate[10]. Additionally, Doğan and Dehghanpour demonstrated that forming a hydrophobic layer on mortar surfaces using silicon-based TiO_2, ZnO, and Recycled Nano Carbon Black (RNCB) decreases surface porosity by optimizing the microstructure and improving hydrophobic characteristics[1].

Motivated by these findings, the present study develops hydrophobic concrete coatings using organosilicone-based materials combined with biosynthesized TiO_2 nanoparticles and coconut-shell-derived carbon as additives. The TiO_2 nanoparticles were synthesized following the method reported by Wellia et al., utilizing 10% v/v *Aloe vera* (L.) Burm. f. peel extract as a green reducing agent to ensure environmentally friendly synthesis while employing simpler equipment under ambient conditions, without the need for high temperatures or pressures[11].

2. Materials and Methods

2.1. Materials

The materials used in this study are Portland Cement I (Semen Padang), sand, coconut shell, deionized water (Waterone), distilled water, 70% ethanol, Organosilicone, $TiCl_4$ 1 M (Merck), and *Aloe vera* (L.) Burm. f.

2.2. Instruments

The instruments used in this study are glassware, analytical balance, magnetic stirrer, filter paper (Whatman), oven (Memmert), centrifuge, pH-meter (B-MAX), hot plate (AGIMATIC REV-E), sonicator, brush and sample mold. The characterization instruments used were SEM-EDX (JEOL JSM-6360), XRD (XPERT PRO PANalytical PW 30/40), XRF (PANalytical Epsilon 3), FTIR (PerkinElmer), and water contact angle meter.

2.3. Synthesis

2.3.1. Concrete Sample Preparation

Concrete samples were made with a cement:sand:gravel mix ratio of 1:2:3. The concrete mixture was molded with 30 mm^3 sample molds and cured for 28 days.

2.3.2. Coconut Shell Charcoal Fabrication

The collected coconut shells were washed and cleaned from the skin and then dried. The shell were then burned to form charcoal. The resulting product is pulverized to form carbon powder.

2.3.3. Preparation of *Aloe vera* (L.) Burm. F

Aloe vera (L) Burm. f. was taken and separated from the gel. 10 g fresh *Aloe vera* (L.) Burm. f. bark was washed and pulverized. The *Aloe vera* (L.) Burm. f. bark was heated in 100 mL of deionized water for 1 hour at 70 ºC. The *Aloe vera* (L) Burm. f. extract was filtered using Whatman filter paper.

2.3.4. Biosynthesis of TiO_2 Nanoparticles

In the biosynthesis of TiO_2 nanoparticles, titanium chloride solution (1 M, $TiCl_4$) was prepared in 100 mL of deionized water and *Aloe vera* (L) Burm f. extract was added dropwise under a constant stirring speed. Then, 1 M NaOH was added until pH 7 and continued with constant stirring for 24 hours. Nanoparticles formed during the synthesis process were collected by centrifugation (10,000 rpm) and washed repeatedly with ethanol. The nanoparticles were washed again with distilled water, dried at 100 ºC for 10 hours, and calcined at 500 ºC for 1 hour.

2.3.5. Preparation of Hydrophobic Coating

TiO_2 was synthesized in a glass cup, each sample was made into 4 variations based on mass addition (0.10 g, 0.15 g, 0.20 g, and 0.25 g). Furthermore, 2 mL of Organosilicone was added to each glass cup and then dispersed with a sonicator for 15 minutes. The hydrophobic solution formed was applied once to the surface of the concrete sample with a brush. The hydrophobic coating on the concrete sample was dried for 24 hours at 50 °ºC. The same steps were carried out for carbon addition as in Table 1.

Table 1. Sample and sample code

Sample code	TiO_2 (g)	Carbon (g)	Organosilicone (mL)
Concrete (concrete)	-	-	-
B/Organosilicone	-	-	2
B/Organosilicone/TiO_2-1	0,10	-	2
B/Organosilicone/TiO_2-2	0,15	-	2
B/Organosilicone/TiO_2-3	0,20	-	2
B/Organosilicone/TiO_2-4	0,25	-	2
B/Organosilicone/C-1	-	0,10	2

B/Organosilicone/C-2	-	0,15	2
B/Organosilicone/C-3	-	0,20	2
B/Organosilicone/C-4	-	0,25	2

3. Results and Discussion

3.1. Surface Morphology

The microstructures of the sample surface obtained from SEM are shown in Figure 1 (a-j). The untreated concrete surface (Figure 1 (a)) is irregular and pore-rich, leading to easy water diffusion on the concrete surface. On the surface of concrete coated with organosilicone (Figure 1 (b)), there is a reduction in porosity on the concrete surface, thereby reducing water absorption. Al-Kheetan et al. stated that silicone-based compounds prevent water diffusion from the porous structure of cement-based materials and increase the resistance of hydrophobic materials[12].

The surface morphology of hydrophobic concrete with TiO_2 nanoparticles used in different ratios is shown in Figure 1 (c-f). The concrete surface is flatter and the roughness on the surface of the material is relatively more uniform with the addition of 0.20 g TiO_2 (Figure 1(e)) compared to the addition of 0.10 g and 0.15 g TiO_2. Doğan and Dehghanpour state that the addition of TiO_2 particles in the preparation of hydrophobic coatings forms a protective layer preventing water absorption on the surface of cement-based materials with good durability and workability[1]. In contrast, the rough structure seen in Figure 1 (f) indicates that agglomerates are formed in the microstructure of samples with greater TiO_2 concentration. The nanoparticles are unevenly distributed in the form of aggregates that cannot provide a uniform structure on the concrete surface, resulting in a lower hydrophobicity contribution.

When the morphology of the hydrophobic surface prepared by adding carbon particles on the concrete surface is examined, it can be seen that the distribution of particles in low amounts (0.10 g) is relatively uneven. When the amount of particles is increased to 0.20 (Figure 1(i)), the carbon particles form a dense structure with increased regular distribution on the concrete surface. Shahbazi et al. reported that micro-scale carbon particles create a rough surface, thereby leading to higher hydrophobic properties[4]. Thus, it can be stated that carbon used with Organosilicone provides good hydrophobicity and can be used to protect concrete surfaces.

As a result of the irregular distribution of the high number of particles in the B/Organosilicone/C-4 sample (Figure 1(j)), it is observed that the particles in the coating morphology are agglomerated. The uneven distribution observed on the coating surface can be explained by the tendency of particles with large grain sizes to agglomerate due to their small surface area[1].

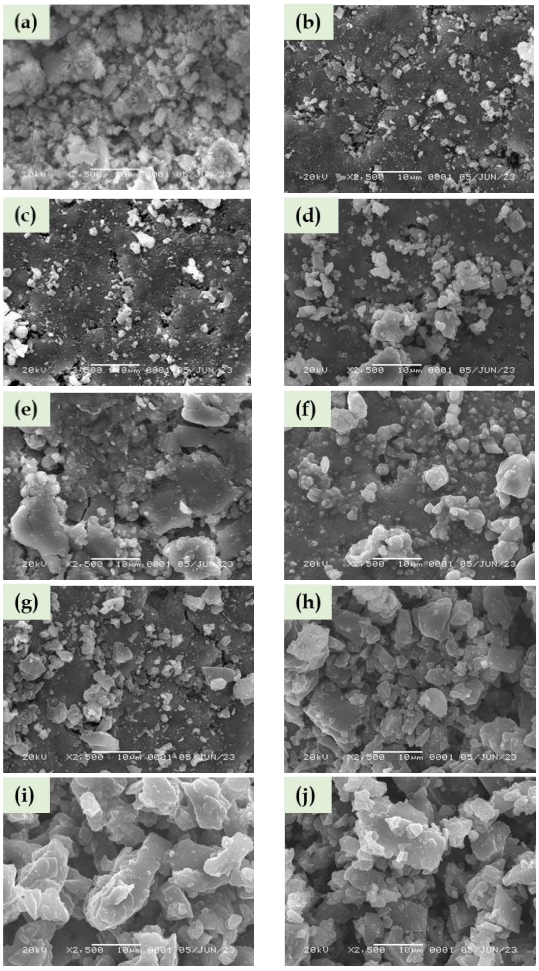


Figure 1. Hydrophobic surface; (a) Concrete, (b) B/Organosilicone, (c) B/Organosilicone/TiO_2-1, (d) B/Organosilicone/TiO_2-2, (e) B/Organosilicone/TiO_2-3, (f) B/Organosilicone/TiO_2-4, (g) B/Organosilicone/C-1, (h) B/Organosilicone/C-2, (i) B/Organosilicone/C-3 and (j) B/Organosilicone/C-4

3.2. Elemental Composition

The EDS of the untreated concrete surface in Figure 2 (a) detected elements such as Al, K, Fe, Si, O, and Ca. The peak of Ca decreased on the surface of the B/Organosilicone/TiO_2 and B/Organosilicone/C samples compared to the untreated concrete samples. This indicates that the hydrophobic layer has been successfully distributed on the surface thus improving the surface performance of the material as reported by Lian et al[13].

Figure 2 (b) shows the EDS analysis of the hydrophobic surface of sample B/Organosilicone/TiO_2, the peak intensities of Ti, O, Si, and Ca are observed on the concrete surface. In the EDS analysis of the surface of the hydrophobic layer of sample B/Organosilicone/C, as shown in Figure 2 (c), the peaks of Si, O, Ca, and C are observed on the concrete surface. The decrease of the Ca

peak and the increase of C and Si peaks are attributed to the concentration of these elements in the hydrophobic coating. In the EDS analysis results of the surface of B/Organosilicone/TiO_2 and B/Organosilicone/C samples, elements such as Al, K, and Fe were not detected. This finding indicates that the applied hydrophobic coating covers the surface, reduces porosity and improves the hydrophobicity of the concrete surface.

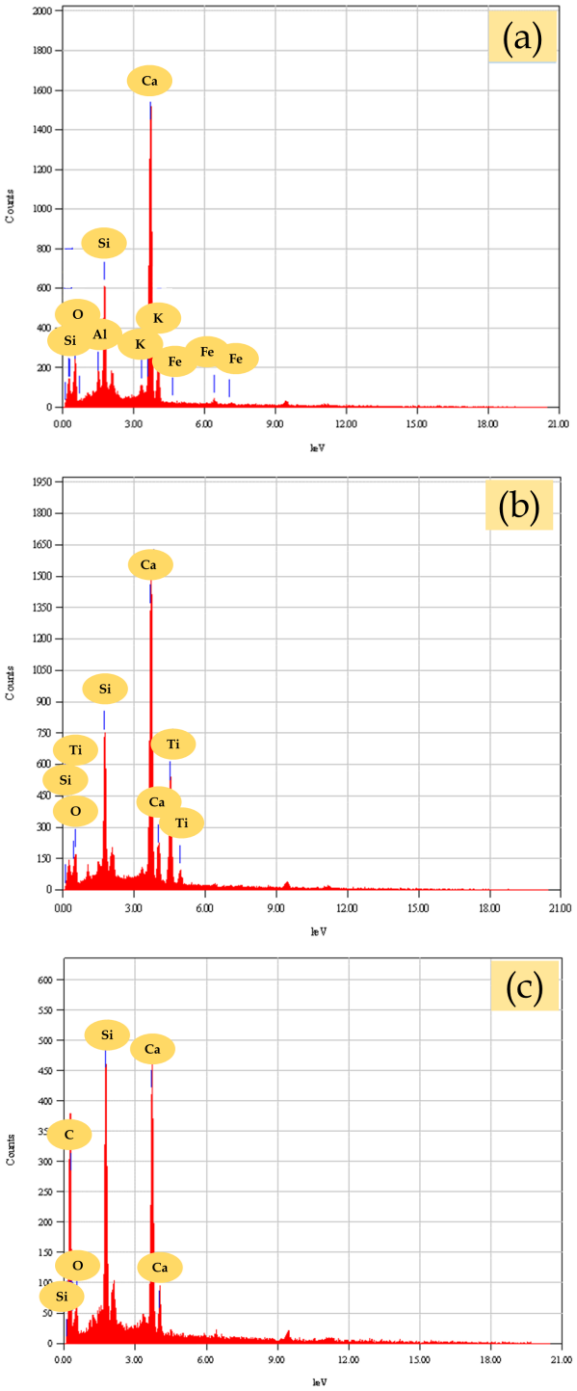


Figure 2. EDS spectra of the sample surface; (a) Concrete, (b) B/Organosilicone/TiO_2 and (c) B/Organosilicone/C

3.3. Crystal Phase

The result of XRD characterizations are shown in Figure 3. The diffraction peaks of Quartz-SiO_2 and Calcite-$CaCO_3$ were observed in the untreated concrete samples. While in the B/Organosilicone sample, a higher Quartz-SiO_2 diffraction peak and a decrease in the Calcite-$CaCO_3$ diffraction peak were observed when compared to untreated concrete due to the presence of an organosilicone layer on the concrete surface.

In the B/Organosilicone/TiO_2 sample, the relatively high Quartz-SiO_2 diffraction peak compared to the B/Organosilicone/C sample explains the role of the hydrophobic layer on the concrete surface covering defects such as porosity. The B/Organosilicone/TiO_2 sample also shows diffraction peaks at (101), (112), and (200) with diffraction angles (2θ) of 25.1°, 37.3° and 47.7° which correspond to the anatase phase of TiO_2 based on ICSD standard No. 44882. In the B/Organosilicone/C sample, unclear diffraction peaks were observed indicating amorphous carbon. Then, the decrease in the Calcite-$CaCO_3$ peak in the B/Organosilicone/TiO_2 and B/Organosilicone/C samples can be attributed to a decrease in the permeability of the concrete surface[1].

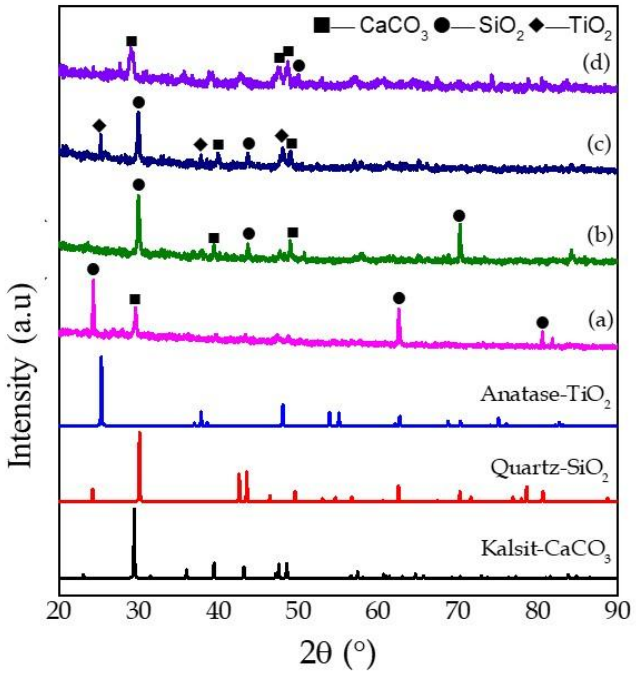


Figure 3. XRD pattern of (a) Concrete, (b) B/Organosilicone (c) B/Organosilicone/TiO_2 and (d) B/Organosilicone/C

3.4. Fourier Transform Infrared (FTIR) Analysis

The results of the FTIR spectrum data analysis can be seen in Figure 4. Absorption bands at several wave numbers are clearly visible. The presence of absorption bands at wave number 2963 cm^{-1} in B/Organosilicone, B/Organosilicone/C, and 2965 cm^{-1} in B/Organosilicone/TiO_2

samples is given in Table 2. The presence of aliphatic C-H from the organosilicone used which is not found in untreated concrete samples. The absorption bands at wave numbers of 1405, 1411, 1407, and 1404 cm^{-1} observed in all spectra can prove the presence of $CaCO_3$[14]. However, of the four absorption bands, wave number of 1405 cm^{-1} (untreated concrete) has a higher intensity than the other samples.

In Figure 4, the absorption bands at wave numbers 1260 cm^{-1} and 1258 cm^{-1} indicate the presence of O-Si-O from Organosilicone but are not visible in the FTIR spectra of untreated concrete samples. The appearance of absorption bands at 1002, 992, 1009, and 1014 cm^{-1} indicates the presence of Si-O in all spectra derived from concrete samples. At wave numbers of 870, 874, 871 and 867 cm^{-1} which can be observed in all spectra indicates the presence of CO_3^{2-}. The wave numbers of 450, 459, and 453 cm^{-1} are assigned to O-Si-O bond vibrations, where the intensity of the absorption bands in B/Organosilicone/TiO_2 and B/Organosilicone/C decreases indicating the presence of Ti-O and carbon on the surface of the samples . Then, the absorption band at wave number 477 cm^{-1} proves the presence of Ti-O bond vibrations in the B/Organosilicone/TiO_2 sample.

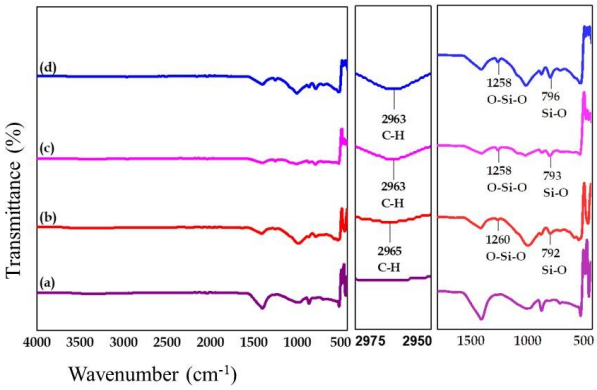


Figure 4. FTIR spectrum of (a) Concrete, (b) B/Organosilicone, (c) B/Organosilicone/TiO_2 and (d) B/Organosilicone/C

Table 2. FTIR Spectrum Interpretation

Wave Numbers (cm^{-1})				Interpretation
Concrete	B/Organosilicone	B/Organosilicone/TiO_2	B/Organosilicone/C	
-	-	2963	2963	2800 - 2900/ Aliphatic C-H
1405	1411	1404	1407	1300 - 1700/ Asymmetric stretching vibration of CO_3^{2-}
-	1260	1258	1258	950-1260/Si-O
1002	992	1014	1009	970 - 1100/ Asymmetric stretching vibration of Si-O
870	874	867	871	842 - 910/ Asymmetric bending vibration of CO_3^{2-}
-	792	796	793	420 - 780/ Internal bending vibration of Si-O
450	459	453	453	450 - 470/ Binding vibration of O-Si-O
-	-	477	-	400 - 500/ Ti-O Vibration

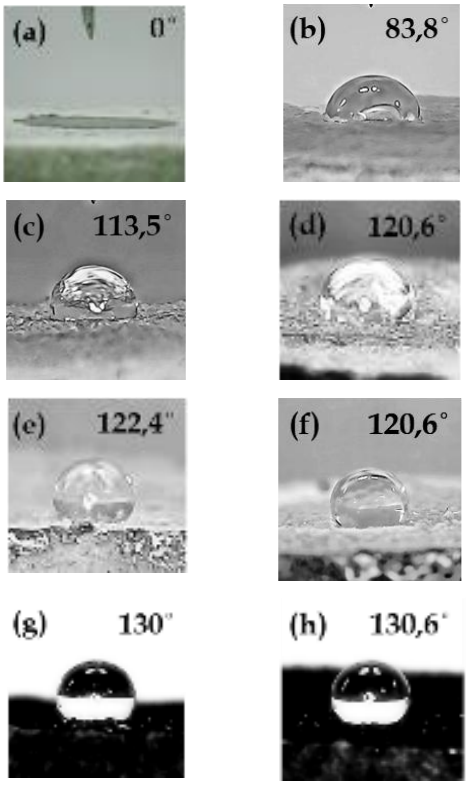
3.5. Water Contact Angle of Hydrophobic Layer

The contact angle of a liquid droplet is a convenient way to describe the wetting properties of a surface. The contact angle is defined as the angle at which the baseline of the droplet and the tangent of the droplet meet. Surfaces that exhibit a water contact angle of less than 90º are called hydrophilic, contact angles of 90º - 120º for hydrophobic surfaces while surfaces with contact angles greater than 150º are called superhydrophobic[15].

The optical micrographs of the samples whose surfaces were coated with Organosilicone-based hydrophobic coatings with the addition of particles (TiO_2 and carbon) of varying mass are shown in Figure 5 (a-j). The water contact angle increased significantly from 0º to 83.8º on the concrete surface without treatment and after coating with Organosilicone (Figure 5 (a,b)). This is because Organosilicone reduces the surface energy with the presence of aliphatic C-H in Organosilicone which is nonpolar[16]. Furthermore, with the addition of 0.10 g and 0.15 g TiO2, the water contact angle increased to 113.5º and 120.6º. With the addition of 0.20 g TiO_2, the water contact angle increased to 122.4º and then decreased to 120.6º at the addition of 0.25 g TiO_2 (Figure 5 (c-f)). A high water contact angle indicates an increase in the hydrophobicity of the sample, so it can be said that TiO_2 nanoparticles can fill micropores and reduce the movement of water to inhibit water diffusion[1]. Increasing surface roughness of concrete with the addition of TiO_2 nanoparticles and decreasing the surface energy caused by organosilicone produce a hydrophobic surface. As for the

decreased water contact angle in sample B/Organosilicone/TiO_2-4, it is caused by the poor distribution of TiO_2 nanoparticles[1].

The contact angle of water on the concrete surface in samples made with the addition of organosilicone-based carbon particles is shown in Figure 5 (g-j). The contact angles of the carbon samples are 130º (B/Organosilicone/C-1), 130.6º (B/Organosilicone/C-2), 138.3º (B/Organosilicone/C-3), and 132.5º (B/Organosilicone/C-4). The results obtained show that carbon particles provide hydrophobic properties on the concrete surface and the water contact angle of the surface of the B/Organosilicone/C sample is higher than that of the B/Organosilicone/TiO_2 sample. The layer formed by carbon and silica particles on the surface of concrete samples acts as a barrier against water diffusion. On the other hand, the addition of large amounts of carbon to a hydrophobic solution shows that the coating formed does not improve the hydrophobic properties of the material for the better [1]. This implies that the water contact angle may decrease in the presence of excessive amounts of carbon particles. Based on the contact angle measurement results, it is known that the B/Organosilicone/TiO_2-3 and B/Organosilicone/C-3 samples have the largest contact angles.



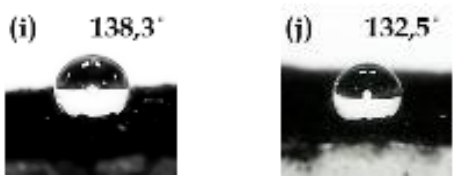


Figure 5. Water contact angles from samples (a) Concrete, (b) B/Organosilicone, (c) B/Organosilicone/TiO_2-1, (d) B/Organosilicone/TiO_2-2, (e) B/Organosilicone/TiO_2-3, (f) B/Organosilicone/TiO_2-4, (g) B/Organosilicone/C-1, (h) B/Organosilicone/C-2, (i) B/Organosilicone/C-3 and (j) B/Organosilicone/C-4

4. Conclusions

The performance of B/Organosilicone/TiO_2 and B/Organosilicone/Carbon hydrophobic coatings has been evaluated. The addition of biosynthesized TiO_2 nanoparticles and carbon particles from coconut shell waste to the hydrophobic coating increases the surface roughness, thereby increasing the hydrophobicity of the concrete surface. This is evidenced by the contact angle of the B/Organosilicone/TiO_2 sample reaching 122.4º (TiO_2 - 0.20 g) and the B/Organosilicone/C sample up to 138.3º (carbon - 0.20 g). The distribution of particles on the concrete surface in low amounts (0.10 g and 0.15 g) is relatively uneven. The high particle distribution (0.25 g) tends to form agglomerated particles, which can reduce the surface hydrophobicity. Thus, the effectiveness of using carbon in increasing surface hydrophobicity is viewed from the magnitude of the contact angle of the hydrophobic layer. This makes carbon from coconut shell waste can be used as an alternative in hydrophobic surface applications..

Acknowledments

The authors would like to thank all parties involved who contributed in the form of advice, guidance, and counsel, enabling the compilation of this article properly.

Author contributions

Conceptualization: D.V.W
Data curation: R.Y
Formal Analysis: R.Y, D.V.W, B.H
Funding acquisition: R.Y
Investigation: R.Y
Methodology: D.V.W, B.H
Project administration: R.Y.
Resources: D.V.W
Software: R.Y.
Supervision: D.V.W, B.H
Validation: R.Y, D.V.W, B.H.
Visualization: R.Y

Writing – original draft: R.Y, D.V.W
Writing – review & editing: D.V.W, B.H

Conflict of interest

The authors declare no conflict of interest.

References

[1] F. Doğan, H. Dehghanpour, Characterization and hydrophobic surface study of silicon-based TiO_2, ZnO and recycled carbon additives on cementitious materials surface, J. Build. Eng. 40 (2021). https://doi.org/10.1016/j.jobe.2021.102689.

[2] S.S. Ray, P.R.T. Peddinti, R. Soni, B. Kim, Y.I. Park, I.C. Kim, C.Y. Lee, Y.N. Kwon, Effectiveness of nanoparticles-based ultrahydrophobic coating for concrete materials, J. Build. Eng. 66 (2023). https://doi.org/10.1016/j.jobe.2022.105799.

[3] B. Zhang, Q. Li, X. Niu, L. Yang, Y. Hu, J. Zhang, Influence of a novel hydrophobic agent on freeze–thaw resistance and microstructure of concrete, Constr. Build. Mater. 269 (2021). https://doi.org/10.1016/j.conbuildmat.2020.121294.

[4] R. Shahbazi, A.H. Korayem, A. Razmjou, W.H. Duan, C.M. Wang, H. Justnes, Integrally hydrophobic cementitious composites made with waste amorphous carbon powder, Constr. Build. Mater. 233 (2020) 117238. https://doi.org/10.1016/j.conbuildmat.2019.117238.

[5] H. Zhang, S. Mu, J. Cai, R. Chen, The impact of carboxylic acid type hydrophobic agent on compressive strength of cementitious materials, Constr. Build. Mater. 291 (2021) 123315. https://doi.org/10.1016/j.conbuildmat.2021.123315.

[6] X. Pan, Z. Shi, C. Shi, T.C. Ling, N. Li, A review on concrete surface treatment Part I: Types and mechanisms, Constr. Build. Mater. 132 (2017) 578–590. https://doi.org/10.1016/j.conbuildmat.2016.12.025.

[7] A.J. Haider, Z.N. Jameel, I.H.M. Al-Hussaini, Review on: Titanium dioxide applications, Energy Procedia. 157 (2019) 17–29. https://doi.org/10.1016/j.egypro.2018.11.159.

[8] E.H. Sujiono, D. Zabrian, Zurnansyah, Mulyati, V. Zharvan, Samnur, N.A. Humairah, Fabrication and characterization of coconut shell activated carbon using variation chemical activation for wastewater treatment application, Results Chem. 4 (2022) 100291. https://doi.org/10.1016/j.rechem.2022.100291.

[9] C.O. Umerah, D. Kodali, S. Head, S. Jeelani, V.K. Rangari, Synthesis of carbon from waste coconutshell and their application as filler in bioplast polymer filaments for 3D printing, Compos. Part B Eng. 202 (2020) 108428. https://doi.org/10.1016/j.compositesb.2020.108428.

[10] Y.G. Zhu, S.C. Kou, C.S. Poon, J.G. Dai, Q.Y. Li, Influence of silane-based water repellent on the durability properties of recycled aggregate concrete, Cem. Concr. Compos. 35 (2013) 32–38. https://doi.org/10.1016/j.cemconcomp.2012.08.008

[11] D.V. Wellia, M.R. Habibillah, A. Syafawi, R. Rahmadini, R. Rahmayeni, N. Pratiwi, A New Combination Method of N-doped TiO_2 Nanoparticles Synthesis for Heavy Metal Ions Cr(VI) Photoreduction Applications, J. Kim. Sains Dan Apl. 26 (2023) 70–78. https://doi.org/10.14710/jksa.26.2.70-78.

[12] M.J. Al-Kheetan, M.M. Rahman, D.A. Chamberlain, Fundamental interaction of hydrophobic materials in concrete with different moisture contents in saline environment, Constr. Build. Mater. 207 (2019) 122–135. https://doi.org/10.1016/j.conbuildmat.2019.02.119.

[13] S. Lian, T. Meng, M. Wang, H. Yu, Effect of Nano-SiO2 on the Mechanical Properties, Microstructure, and Hydration Process of Cementitious Materials Incorporating Hydrophobic Admixture, J. Mater. Civ. Eng. 32 (2020). https://doi.org/10.1061/(asce)mt.1943-5533.0003084.

[14] R. Ylmén, U. Jäglid, Carbonation of Portland Cement Studied by Diffuse Reflection Fourier Transform Infrared Spectroscopy, Int. J. Concr. Struct. Mater. 7 (2013) 119–125. https://doi.org/10.1007/s40069-013-0039-y.

[15] L. Ejenstam, Hydrophobic and superhydrophobic coatings for corrosion protection of steel, 2015.

[16] G. Barati Darband, M. Aliofkhazraei, S. Khorsand, S. Sokhanvar, A. Kaboli, Science and Engineering of Superhydrophobic Surfaces: Review of Corrosion Resistance, Chemical and Mechanical Stability, Arab. J. Chem. 13 (2020) 1763–1802. https://doi.org/10.1016/j.arabjc.2018.01.013.